Available online at www.sciencedirect.com
SCIENCE DIRECT®
Physics Letters A 333 (2004) 347–353
PHYSICS LETTERS A
www.elsevier.com/locate/pla

AC electrokinetics of the microparticles in electrorheological solids

J.P. Huang [a,b,*], K.W. Yu [a]

[a] *Department of Physics, The Chinese University of Hong Kong, Shatin, NT, Hong Kong*
[b] *Max Planck Institute for Polymer Research, Ackermannweg 10, 55128 Mainz, Germany*

Received 9 June 2004; received in revised form 24 October 2004; accepted 25 October 2004

Communicated by R. Wu

Abstract

Under the application of electric fields, the structure of electrorheological (ER) solids can be changed from the body-centered tetragonal lattice (ground state) to other lattices. For a particle in the lattice, we derive its dipole factor by taking into account both the local-field effect arising from all the other particles and the multipolar interaction between two touching particles, through the Ewald–Kornfeld formulation and multiple image method. For simplifying the study, the dipole factors are expressed in the dielectric dispersion spectral representation exactly. It is found that the electrorotation (EOR) spectrum of ER solids can be affected significantly by the structure transformation, and the local-field effect as well as the multipolar interaction. Our results are well understood in the spectral representation theory. Thus, it is possible to monitor the structure of ER solids by detecting the EOR spectrum.

PACS: 77.22.Ej; 82.70.-y; 83.80.Gv

Keywords: AC electrokinetics; Electrorheological solids

1. Introduction

When a suspension of polarizable particles is subject to a strong electric field, the induced dipole moment can order the suspended particles into columns. These suspensions are called electrorheological (ER) fluids [1]. The rapid field-induced aggregation and the large anisotropy of ER fluids render this material potentially important for technological applications [2]. As the external field exceeds a critical electric field, ER fluids turn into a solid, the ground state of which is a body-centered tetragonal (bct) lattice. For the ER solids, one [3] proposed that a structure transformation from the bct ground state to some other lattices

* Corresponding author.
E-mail address: jphuang@alumni.cuhk.net (J.P. Huang).

0375-9601/$ – see front matter
doi:10.1016/j.physleta.2004.10.056

can appear when a magnetic field is simultaneously applied perpendicular to the electric field and the particles have magnetic dipole moments. This proposal was verified experimentally and a structure transformation from the bct to the face-centered cubic (fcc) lattices was observed indeed [4]. Recently, it was further shown that an alternative structure transformation from the bct to the fcc structure can also occur for ER solids through the application of electric fields only [5].

Electrorotation [6] (EOR) is a phenomenon in which an interaction between a rotating ac electric field and suspended dielectric particles leads to a rotational motion of the particles. During the past two decades, the EOR has been increasing employed as a sensitive tool for noninvasive studies of a broad variety of particles [7–10]. Also, we have shown that either local-field effects or multipolar interactions can change the EOR spectrum significantly [11–14].

In this Letter, we shall investigate the EOR of ER solids, by including the local-field effect in the lattices. In fact, we have presented an effective medium theory (EMT) for considering local-field effects on the EOR and dielectric dispersion spectra of colloidal particles [12–14]. Unfortunately, the EMT could not be used to study the detailed structural information. Thus, we shall consider the specific structural information, based on the Ewald–Kornfeld formulation [5,15–17] instead, and compute the local electric field for a particle in ER solids by taking into account the influence of all the other particles. In particular, since in ER solids all the particles are touching, the large mutual polarization interaction is expected to play a role. So, we shall also include the multiple image interaction, by using the multiple image method [18].

2. Formalism

When a spherical particle in an ER solid is subject to a rotating electric field, the EOR velocity of the particle $\Omega(f)$ is given by [6]

$$\Omega(f) = -F\,\mathrm{Im}[\text{Dipole factor}], \tag{1}$$

where F is a function of the real dielectric constant of the host fluid ϵ_2, the viscosity of the host ξ, and the strength of the external rotating electric field E_0. Here Im$[\cdots]$ denotes the imaginary part of $\cdots$. Eq. (1) can be considered as an approximation, due to two reasons: (a) The electrical torque on an isolated particle is proportional to the imaginary part of the dipole factor (also called Clausius–Mossotti factor) as the particle is subjected to a homogeneous rotating electric field. The electric field on the particle in the lattice of interest is highly inhomogeneous. The torque in this situation should be computed from the Maxwell stress tensor applied on the surface of the particle or from a multipolar expansion. (b) The viscous friction of a spherical particle near other particles is a complicated hydrodynamic problem. It is anisotropic and, therefore, the angular velocity will become different along the three spatial directions. In the present Letter, our focus is on the electric torque, in the sense that we account for the local-field effect in a dense solid, and we shall not do anything about the hydrodynamic torque. Most importantly, Eq. (1) indicates that the EOR spectrum under investigation is crucially determined by the imaginary part of the dipole factor whereas the coefficient F that is real serves only as a multiple of the magnitude of the EOR velocity. Hence the calculation of the dipole factor will offer one the exact details on characteristic frequencies at which the EOR velocity reaches maximum, as well as a framework of the EOR spectrum.

2.1. Effect of long-range interactions

2.1.1. Dipole factor

Let us start by considering the ground state of an ER solid, namely a bct lattice. The bct lattice can be regarded as a tetragonal lattice, plus a basis of two particles each of which is fixed with a point dipole at its center. One of the two particles is located at a corner and the other at the body center of the tetragonal unit cell. Its lattice constants are $c = q\zeta$ and $a(=b) = \zeta q^{-1/2}$ along the z- and x- (y-) axes, respectively. The volume of the tetragonal unit cell keeps the same, $V_c = \zeta^3$, as q varies. Therefore, the degree of anisotropy of the lattice is given by how q is deviated from unity. In this case, the uniaxial anisotropic axis has been directed along z axis.

To induce the EOR of the particles, we apply an external electric field $\mathbf{E}_0$ in xy-plane. In this case, the dipole moments, $\mathbf{P} = P\hat{x} = P\hat{y}$, are perpendicular to the uniaxial anisotropic axis. Then, the local field $\mathbf{E}$ (e.g., $\mathbf{E} = E_x\hat{x}$, $E_z = 0$) at the lattice point $\mathbf{R} = \mathbf{0}$ has

the following Ewald–Kornfeld form [5,15–17]

$$E_x = P\sum_{j=1}^{2}\sum_{\mathbf{R}\neq\mathbf{0}}\left[-C_1(R_j)+x_j^2q^2C_2(R_j)\right] - \frac{4\pi P}{V_c}\sum_{\mathbf{G}\neq\mathbf{0}}S(\mathbf{G})\frac{G_x^2}{G^2}\exp\left(\frac{-G^2}{4\eta^2}\right)+\frac{4P\eta^3}{3\sqrt{\pi}}. \tag{2}$$

In this equation, C_1 and C_2 are two coefficients, $C_1(r) = \operatorname{erfc}(\eta r)/r^3 + 2\eta/(\sqrt{\pi}r^2)\exp(-\eta^2r^2)$ and $C_2(r) = 3\operatorname{erfc}(\eta r)/r^5 + [4\eta^3/(\sqrt{\pi}r^2) + 6\eta/(\sqrt{\pi}\times r^4)]\exp(-\eta^2r^2)$, where $\operatorname{erfc}(\eta r)$ denotes the complementary error function, and η an adjustable parameter making the summation converge rapidly. In Eq. (2), R and G are the lattice vector and the reciprocal lattice vector, respectively, $\mathbf{R} = \zeta(q^{-1/2}l_1\hat{x}+q^{-1/2}l_2\hat{y}+ql_3\hat{z})$ and $\mathbf{G} = 2\pi/\zeta(q^{1/2}u_1\hat{x}+q^{1/2}u_2\hat{y}+q^{-1}u_3\hat{z})$, where $l_1, l_2, l_3, u_1, u_2, u_3$ are integers. In addition, x_j and R_j are respectively given by $x_j = l-(j-1)/2$ and $R_j = |\vec{R}-(j-1)/2(a\hat{x}+a\hat{y}+c\hat{z})|$, and the structure factor $S(\mathbf{G})$ is $S(\mathbf{G}) = 1+\exp[i(u+v+w)/\pi]$.

Next, let us apply the result of the local field (Eq. (2)) to evaluate the dipole factor $\tilde{b}'$ of the particle in the lattice via a self-consistent method, thus yielding

$$\tilde{b}' = \frac{\tilde{b}}{1-\tilde{b}\rho\beta_x'}, \tag{3}$$

where ρ stands for the volume fraction of the particles, and $\beta_x' = 3E_xV_c/4\pi P$ the local field factor, which was measured in computer simulations [19]. We shall use β_z' and β_x' to denote the local-field factors parallel and perpendicular to the uniaxial anisotropic axis, respectively, which are both a function of the degree of anisotropy q. Note that $\beta_z' = \beta_x' = 1$ for bcc lattice, namely $q = 1$. Furthermore, there exists a sum rule for β_z' and β_x', namely $2\beta_x'+\beta_z' = 3$ [20]. In Eq. (3), $\tilde{b}$ denotes the dipole factor for an isolated particle, namely

$$\tilde{b} = \frac{\tilde{\epsilon}_1-\tilde{\epsilon}_2}{\tilde{\epsilon}_1+2\tilde{\epsilon}_2}, \tag{4}$$

where the complex dielectric constant $\tilde{\epsilon}_N = \epsilon_N + \sigma_N/i2\pi f$, with $N = 1, 2$ for the particles and host, respectively. Here ϵ denotes the real dielectric constant, σ the conductivity, f the frequency of the field, and $i = \sqrt{-1}$. From Eq. (4), it is shown that $\tilde{b}' \to \tilde{b}$ as $\rho \to 0$ (e.g., $\rho = 0.02$ used in Fig. 2). In other words, as $\rho \to 0$, the case of an isolated particle is reproduced through Eq. (4), as expected.

2.1.2. Dielectric dispersion spectral representation

For simplifying the study, we resort to the dielectric dispersion spectral representation (DDSR) approach [13], in an attempt to derive the dielectric strength and the characteristic frequency at which the EOR velocity reaches maximum. After introducing a real dielectric constant ratio $s = (1-\epsilon_1/\epsilon_2)^{-1}$ and real conductivity ratio $t = (1-\sigma_1/\sigma_2)^{-1}$, we re-express $\tilde{b}'$ (Eq. (3)) in the DDSR as

$$\tilde{b}' = b' + \frac{\Delta\epsilon}{1+if/f_c}, \tag{5}$$

with $b' = -1/[3s-(1-\rho\beta')]$. Here, the dielectric strength $\Delta\epsilon$ and the characteristic frequency f_c are, respectively, given by

$$\Delta\epsilon = \frac{t-s}{[3t-(1-\rho\beta')][3s-(1-\rho\beta')]}, \tag{6}$$

$$f_c = \frac{1}{2\pi}\frac{\sigma_2 s[3t-(1-\rho\beta')]}{\epsilon_2 t[3s-(1-\rho\beta')]}. \tag{7}$$

So far, in Eq. (5) we have taken into account the local-field effect due to all other particles in the lattice of interest and also expressed the dipole factor in the DDSR exactly.

2.2. Effect of multiple images

2.2.1. Dipole factor

In the lattice all the particles are touching, and hence the large mutual polarization interaction is expected to play a role. Recently we [11] showed that this interaction is weak enough to be neglected as the center-to-center separation L between the particles is larger than $2D$ (here D denotes the diameter of the particle).

Now let us include the multiple image interaction between a pair of touching particles in xy-plane, by using the multiple image method [18]. When the two particles are subjected to an external uniform electric field, a dipole moment is induced into each particle. Let us denote the dipole moment of particles A and B as P_{A0} and P_{B0} ($\equiv P_{A0}$), respectively. Then we consider the image effect. The dipole moment P_{A0} induces an image dipole P_{A1} into particle B. Next, P_{A1} yields another image dipole P_{A2} into particle A. As a

result, multiple images are formed. The same description holds for P_{B0}. Therefore, we obtain the infinite series of image dipoles. To this end, we obtain the sum of the dipole moment inside each particle, and then the desired expressions for the dipole factor are obtained. Consider two basic cases: longitudinal field where the field is parallel to the line joining the centers of the particles, and transverse field where the field is perpendicular to the line joining the centers of the particles. Based upon the multiple image method [18], the dipole factor $\tilde{b}'^{*}_{(p)}$ is given by

$$\tilde{b}'^{*}_{(p)} = \tilde{b}' \sum_{n=0}^{\infty} (p\tilde{b}')^n \left(\frac{\sinh\alpha}{\sinh(n+1)\alpha} \right)^3, \tag{8}$$

where the polarization index $p = 2$ ($p = -1$) denotes longitudinal (transverse) field cases, and α satisfies $\cosh\alpha = L/D$ which denotes the separation between the particles.

In this case, for calculating the EOR spectrum the dipole factor of Eq. (1) should be replaced by $(\tilde{b}'^{*}_{(p=2)} + \tilde{b}'^{*}_{(p=-1)})/2$ which is obtained from the average over all possible orientations of the particles.

2.2.2. Dielectric dispersion spectral representation

Again, let us express $\tilde{b}'^{*}_{(p)}$ (Eq. (8)) in the DDSR. Then, $\tilde{b}'^{*}_{(p)}$ has the exact transformation in terms of an infinite series of dispersion strengths $\Delta\epsilon_m^{(p)}$ and characteristic frequencies $f_{mc}^{(p)}$ as follows

$$\tilde{b}'^{*}_{(p)} = b'^{*}_{(p)} + \sum_{m=1}^{\infty} \frac{\Delta\epsilon_m^{(p)}}{1 + if/f_{mc}^{(p)}}, \tag{9}$$

with

$$b'^{*}_{(p)} = \sum_{m=1}^{\infty} -\frac{4m(m+1)e^{-(1+2m)\alpha}\sinh^3\alpha}{3s - [(1-\rho\beta') - pe^{-(1+2m)\alpha}]},$$

where the dispersion strength $\Delta\epsilon_m^{(p)}$ and the characteristic frequency $f_{mc}^{(p)}$ are given by

$$\begin{aligned}\Delta\epsilon_m^{(p)} = {} & -4m(m+1)e^{-(1+2m)\alpha}\sinh^3\alpha(s-t) \\ & \times \left\{3t - \left[(1-\rho\beta') - pe^{-(1+2m)\alpha}\right]\right\}^{-1} \\ & \times \left\{3s - \left[(1-\rho\beta') - pe^{-(1+2m)\alpha}\right]\right\}^{-1},\end{aligned} \tag{10}$$

$$f_{mc}^{(p)} = \frac{1}{2\pi} \frac{\sigma_2 s\{3t - [(1-\rho\beta') - pe^{-(1+2m)\alpha}]\}}{\epsilon_2 t\{3s - [(1-\rho\beta') - pe^{-(1+2m)\alpha}]\}}. \tag{11}$$

From the physical point of view, the integer m of Eq. (9) means the number of peaks of electrorotation. Generally speaking, due to the existence of multipolar interaction, the number of electrorotation peaks can be infinite, that is, $m \to \infty$. In the next section, we shall show that only the small m plays a crucial role in the electrorotation spectrum (the effect of large m is weak enough to be neglected). In the above derivation, we have used an identity $\sinh^{-3} X = \sum_{m=1}^{\infty} 4m \times (m+1)e^{-(1+2m)X}$.

3. Numerical results

Fig. 1 shows the dependence of the local-field factor β'_x on the degree of anisotropy q. It is evident to find that β'_x increase for increasing q. And a plateau is shown at $\beta'_x = 1$, which actually includes the bcc-to-fcc transformation. Similar plateau also occurs for other parameters (e.g., $\Delta\epsilon$ and f_c, see Fig. 2) due to their dependence on the local-field factor.

Fig. 2 is plotted, in order to show concentration effects on electrorotation spectra. In this figure, both dispersion strengths and characteristic frequencies are displayed. It is worth noting that each electrorotation spectrum can be indicated by using a pair of dispersion strength and characteristic frequency, as respectively expressed in Eqs. (6) and (7). Fig. 2(a) displays the

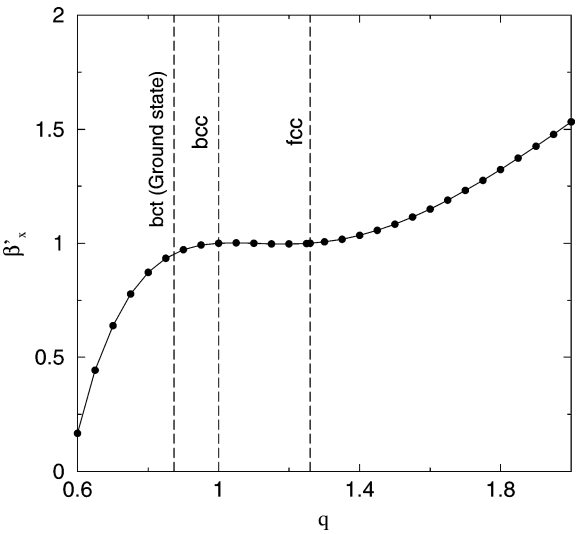

Fig. 1. Local field factor β'_x as a function of the degree of anisotropy q. Also shown are the bct, bcc and fcc lattices which are respectively for $q = 0.87358$, $q = 1.0$ and $q = 2^{1/3}$ (dashed lines).

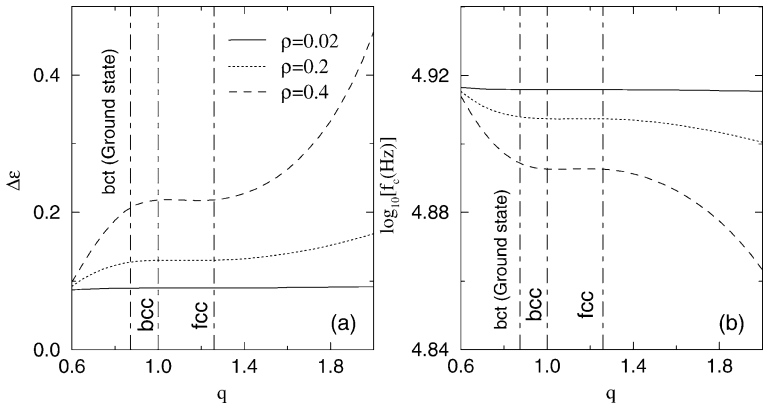

Fig. 2. Dependence of (a) the dispersion strength $\Delta\epsilon$ and (b) the characteristic frequency f_c on q, for various volume fraction ρ at $\sigma_2 = 2.8 \times 10^{-6}$ S/m, $t = -1/90$, $\epsilon_2 = 2.25\epsilon_0$, and $s = -0.045$. Here ϵ_0 denotes the dielectric constant of free space. The bct, bcc and fcc lattices are also shown (dot-dashed lines).

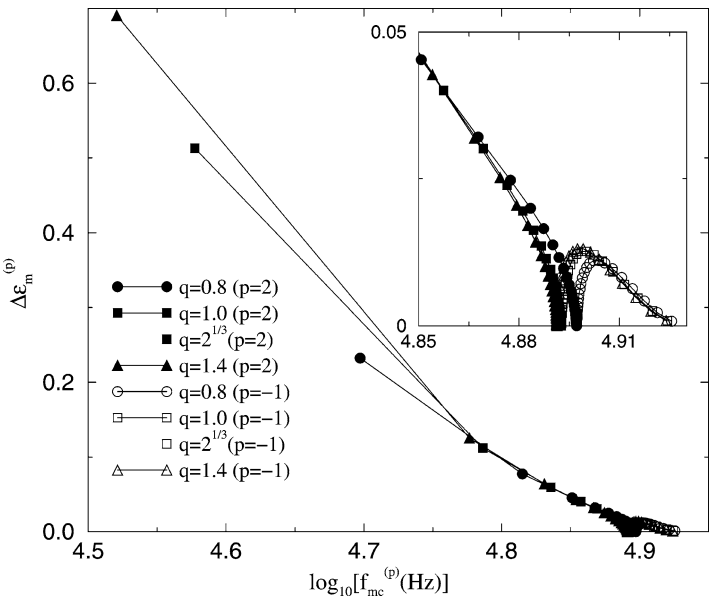

Fig. 3. Dispersion strength versus the characteristic frequency for different degree of anisotropy at $\rho = 0.4$ and $L/D = 1.01$. Note the points for $q = 1.0$ and $q = 2^{1/3}$ are overlapped for $p = 2$ and $p = -1$, respectively. Lines are a guide for the eye.

dependence of the dispersion strength $\Delta\epsilon$ on q. We find that $\Delta\epsilon$ increases for increasing q, which suggests that larger q leads to larger $-\operatorname{Im}[\tilde{b}']$. Also, increasing ρ causes $\Delta\epsilon$ to increase, as indicates that the higher volume fraction of the particles should predict larger $-\operatorname{Im}[\tilde{b}']$ too. In Fig. 2(b), we show the characteristic frequency f_c as a function of q. For increasing q, f_c is caused to decrease. Thus, a red-shift (i.e., a phenomenon that a characteristic frequency is caused to locate at a lower frequency) of the EOR spectrum is expected to appear as q increases. Also, for larger volume fraction, smaller f_c is obtained as well. In other words, the existence of clusters can make electrorotation spectra red-shifted.

In Fig. 3, we investigate the dispersion strength versus the characteristic frequency for different degree of anisotropy by taking $m = 1 \sim 100$. At a given q, for the longitudinal or transverse field case, increasing m leads to sub-dispersions which actually arise from the effect of multiple images. However, for large

m, the dispersion strength tends to zero, that is, the corresponding dielectric dispersion is weak enough to be neglected. In other words, only the small m plays an important role in the EOR spectrum. From Fig. 3, we find that the effect of multiple images or q has a stronger effect on the EOR spectrum for the longitudinal field case than for the transverse field. Moreover, for the longitudinal field case multiple images play a role in the low frequency range. For the transverse field case the behavior is the opposite. In a word, Fig. 3 helps to clarify the interesting question of which polarization mechanism is present. Regarding the infinite number of subdispersion, we would also like to refer to Fig. 5 of the former work [21] in which we plot the dispersion strength versus m and found that these dispersions accumulate at the dipole ones (this is the reason why we could not see separate peaks).

In Fig. 4, we plot the EOR spectrum which is given by the imaginary part of the corresponding dipole factor $-$ Im[Dipole factor]. Note that the curves predicted by $q = 1.0$ (bcc) and $2^{1/3}$ (fcc) are overlapped for the case of the lattice with multiple images, as already predicted in the DDSR, see Fig. 3. By comparing the isolated-particle case with the nonisolated-particle, it is found that the local-field effect causes the EOR peak value to increase. Moreover, as we take into account the multiple images, the peak value is caused to

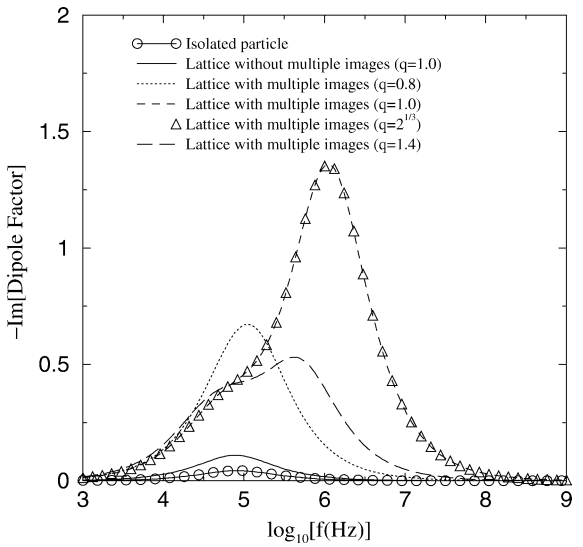

Fig. 4. EOR spectrum given by the imaginary part of the dipole factor. Parameters: $\sigma_2 = 2.8 \times 10^{-6}$ S/m, $t = -1/90$, $\epsilon_2 = 2.25\epsilon_0$, $s = -0.045$, $\rho = 0.4$, and $L/D = 1.01$.

increase again, which is accompanying with the appearance of a sub-dispersion peak. Thus, we should take into account the multiple image effect on the EOR spectrum. In addition, q is also shown to play an important role in the EOR spectrum. In particular, the bcc ($q = 1.0$) [or fcc ($q = 2^{1/3}$)] lattice exhibits the highest peak value as well as characteristic frequency. In fact, most of the results have already been well understood with the aid of the DDSR (see Figs. 2 and 3).

4. Discussion and conclusion

We have discussed the EOR spectrum of the ER solid which is subjected to the structure transformation due to the influence of the local field. Based on the Ewald–Kornfeld formulation and multiple image method, the dipole factor for a particle in the ER solid was analytically derived by including the local-field effect arising from all the other particles, and the multipolar interaction between two touching particles. The dipole factor has been exactly expressed in the DDSR, thus simplifying the study.

As a matter of fact, one of the present authors [22] has applied the multiple image method to treat the ground state of ER solids and compared favorably with the multipolar expansion method [23]. Although there is no simple multiple image method for dielectric spheres, a multiple image method does exist for dielectric spherical particles [24]. Our method is a lot simpler, albeit somewhat approximate. The previous version of Ref. [18] adopted $\tau = (\tilde{\epsilon}_1 - \tilde{\epsilon}_2)/(\tilde{\epsilon}_1 + \tilde{\epsilon}_2)$ rather than $\tilde{b} = (\tilde{\epsilon}_1 - \tilde{\epsilon}_2)/(\tilde{\epsilon}_1 + 2\tilde{\epsilon}_2)$, and thus was accurate at high contrast, while it is poor at low contrast. Now we have always used the $\tilde{b}$ version, which is also quite accurate at low contrast since it compares very well with the integral equation method [25].

It seems difficult to see through the rotating particles deep inside the colloidal crystal. Fortunately, we might observe them indirectly. It is because we do not need to observe all the rotating particles, but we can select some typical ones deep inside the solid, and observe their rotating signals. For instance, we might embed some permanent magnetic moments into these selected particles in such a way that their dielectric properties do not change, while they have a magnetic field emission. The rotating permanent magnet will give rise to a rotating magnetic dipole field and one can detect.

It is also interesting to extend the present work to deal with the interparticle force [18] of ER solids, in an attempt to take into account both local-field and multiple-image effects. On the other hand, we have not included the effect of an intrinsic dispersion within the dielectric particles, which, however, is expected to play a role as well [13]. In this case, the present theory holds as well.

In view of the equilibrium between the electric applied torque and the viscous one, we obtain the factor $F = \epsilon_2 E_0^2/2\xi_e(\xi)$, where the effective viscosity ξ_e is a function of ξ (viscosity of the fluid). The Maxwell–Garnett approximation [26] usually fails for calculating the effective viscosity ξ_e of ER solids, due to the existence of touching particles. We believe that the lubrication theory [27] can shed some light on the effective viscosity of the ER solid. In addition, it is of particular interest to include the lattice effects on the nonlinear ac responses [28] of ER solids, or on the transient responses of ER fluids to square-wave electric fields in steady shear [29]. In view of the variation of the local field versus the degree of anisotropy (see Fig. 1), we can shed some new light on the harmonics generation [30].

Regarding the electrorotation considered in this work, the electrorotational torque is proportional to the *imaginary* part of the dipole factor (Eq. (1)). In contrast, for dielectrophoresis [31], the dielectrophoretic force is proportional to the *real* part of the dipole factor. In this sense, the present formalism should work for the corresponding dielectrophoresis, too. Unfortunately, it seems difficult for dielectrophoretic behaviors to appear because of the close packing of the particles in the lattice of interest.

To sum up, we have discussed the EOR spectrum of ER solids. Our results have been well understood in the DDSR. We have found that the EOR spectrum can be affected significantly by the structure transformation, and the local-field effect as well as the multipolar interaction. Thus, it is possible to monitor the structure of ER fluids by detecting the EOR spectrum.

Acknowledgements

This work was supported by the Research Grants Council of the Hong Kong SAR Government under Project No. CUHK 403303, and by the Alexander von Humboldt foundation in Germany (J.P.H.).

References

[1] T.C. Halsey, Science 258 (1992) 761.
[2] D.J. Klingenberg, MRS Bull. 23 (1998) 30.
[3] R. Tao, Q. Jiang, Phys. Rev. E 57 (1998) 5761; J.P. Huang, Phys. Rev. E 70 (2004) 041403.
[4] W. Wen, N. Wang, H. Ma, Z. Lin, W.Y. Tam, C.T. Chan, P. Sheng, Phys. Rev. Lett. 82 (1999) 4248.
[5] C.K. Lo, K.W. Yu, Phys. Rev. E 64 (2001) 031501.
[6] T.B. Jones, Electromechanics of Particles, Cambridge Univ. Press, Cambridge, 1995.
[7] W.M. Arnold, U. Zimmermann, Z. Naturforsch. C 37 (1982) 908.
[8] F.F. Becker, X.B. Wang, Y. Huang, R. Pethig, J. Vykoukal, P.R.C. Gascoyne, Proc. Natl. Acad. Sci. USA 92 (1995) 860.
[9] G. Fuhr, U. Zimmermann, S. Shirley, Electromanipulation of Cells, CRC Press, Boca Raton, FL, 1996, pp. 259–328.
[10] K.L. Chan, H. Morgan, E. Morgan, I.T. Cameron, M.R. Thomas, Biochim. Biophys. Acta 1500 (2000) 313.
[11] J.P. Huang, M. Karttunen, K.W. Yu, L. Dong, G.Q. Gu, Phys. Rev. E 69 (2004) 051402.
[12] J.P. Huang, K.W. Yu, G.Q. Gu, Phys. Lett. A 300 (2002) 385.
[13] L. Gao, J.P. Huang, K.W. Yu, Phys. Rev. E 67 (2003) 021910.
[14] R.M. Liu, J.P. Huang, Phys. Lett. A 324 (2004) 458.
[15] P.P. Ewald, Ann. Phys. (Leipzig) 64 (1921) 253.
[16] H. Kornfeld, Z. Phys. 22 (1924) 27.
[17] J.P. Huang, Chem. Phys. Lett. 390 (2004) 380.
[18] K.W. Yu, J.T.K. Wan, Comput. Phys. Commun. 129 (2000) 177.
[19] J.E. Martin, R.A. Anderson, C.P. Tigges, J. Chem. Phys. 108 (1998) 3765.
[20] L.D. Landau, E.M. Lifshitz, L.P. Pitaevskii, Electrodynamics of Continuous Media, second ed., Pergamon, New York, 1984, Chapter II.
[21] J.P. Huang, K.W. Yu, G.Q. Gu, Phys. Rev. E 65 (2002) 021401.
[22] H. Sun, K.W. Yu, Phys. Rev. E 67 (2003) 011506.
[23] H.J.H. Clercx, G. Bossis, Phys. Rev. E 48 (1993) 2721.
[24] T.C. Choy, A. Alexopoulos, M.F. Thorpe, Proc. R. Soc. London, Ser. A 454 (1998) 1993.
[25] J.T.K. Wan, PhD thesis, Chinese University of Hong Kong, Hong Kong, 2001.
[26] T.C. Choy, Physica A 221 (1995) 263.
[27] R.T. Bonnecaze, J.F. Brady, J. Chem. Phys. 96 (1992) 2183.
[28] O. Levy, D.J. Bergman, D. Stroud, Phys. Rev. E 52 (1995) 3184.
[29] Z.W. Wang, Z.F. Lin, H.P. Fang, R.B. Tao, J. Appl. Phys. 83 (1998) 1125.
[30] P.M. Hui, C. Xu, D. Stroud, Phys. Rev. B 69 (2004) 014202.
[31] H.A. Pohl, Dielectrophoresis, Cambridge Univ. Press, Cambridge, 1978.